

**Formation of  $\text{H}_2^+$  and  $\text{H}_3^+$  in energetic highly-charged-ion collisions with  $\text{NH}_3$** Pragya Bhatt,<sup>1,\*</sup> T. Sairam,<sup>1</sup> Ajit Kumar,<sup>2</sup> Herendra Kumar,<sup>3</sup> and C. P. Safvan<sup>1</sup><sup>1</sup>*Inter-University Accelerator Center, Aruna Asaf Ali Marg, New Delhi 110067, India*<sup>2</sup>*Department of Physics, Jamia Millia Islamia, New Delhi 110025, India*<sup>3</sup>*Department of Physics and Astrophysics, University of Delhi, Delhi 110007, India*

(Received 16 May 2017; published 24 August 2017)

The dissociation of  $\text{NH}_3$  is studied using energetic  $\text{H}^+$  and  $\text{Ar}^{q+}$  ( $q = 1, 8$ ) ions. The multi-ion coincidence technique along with the time- and position-sensitive measurements of the recoil ions allows us to distinguish different dissociation channels involving the rearrangement of hydrogen atoms. It is observed that the bond dissociation of  $\text{NH}_3^{x+}$  ( $x = 3-5$ ) occurs in a concerted manner and nonplanar dissociation exists. Our results indicate a competition between the bond-rearrangement and Coulomb repulsion processes in  $\text{NH}_3^{x+}$ . *Ab initio* intrinsic reaction coordinate calculations are performed to understand the bond-rearrangement process in  $\text{NH}_3^{2+}$ .

DOI: [10.1103/PhysRevA.96.022710](https://doi.org/10.1103/PhysRevA.96.022710)**I. INTRODUCTION**

Migration of protons is considered a key process in the isomerization of molecules during chemical reactions both in a solution [1–3] and the gas phase [4–6]. The high mobility of protons has been observed in dications at ultrafast time scales along the potential-energy surface (PES) [7]. Studying proton migration and the formation of  $\text{H}_2^+$  and  $\text{H}_3^+$  ions is also significant from an astrophysical point of view [8]. The origin of the dominant presence of molecular hydrogen in astronomical environments (mainly in diffuse clouds where the particle density is very low) is still a debatable issue. The formation of stars and the evolution of galaxies are thought to be led by molecular hydrogen. The  $\text{H}_3^+$  ion, being a universal proton donor, is considered a key intermediate in the chemistry of formation of many complex molecular species in the interstellar medium [9]. The existence of hydrogen-containing molecules like  $\text{H}_2\text{O}$ ,  $\text{CH}_4$ ,  $\text{NH}_3$ , and several other hydrocarbons is explained by the protonation of atomic species like oxygen, carbon, nitrogen, etc., by  $\text{H}_3^+$  [9,10]. These observations have led to the extensive study of the processes involving the rearrangement of hydrogen atoms [11–19], for example, in water [15,18], hydrocarbons [6,11,14,16,18], and alcohol molecules [20,21]. However, there are very few experimental reports on the bond-rearrangement and dissociation processes in  $\text{NH}_3$ , despite its importance in the pharmaceutical industry, chemical synthesis processes, and astrophysics. The detection of amino acids, the building blocks of proteins, in interstellar objects is suggested as being due to the reactions and associations between small molecules in the presence of  $\text{NH}_3$  [9]. Winkoun and Dujardin [22] studied the dissociation of  $\text{NH}_3^{2+}$  using synchrotron radiation at energies of 35–49 eV. Jochim *et al.* [17] have reported bond rearrangement in  $\text{NH}_3$  under energetic proton impact. Theoretical studies on bond rearrangement in  $\text{NH}_3$  are scarce [17].

We have chosen  $\text{NH}_3$  to study the rearrangement of H atoms considering its trigonal pyramidal shape. The repulsion caused by the presence of a lone pair at a N atom further enhances the probability of interaction among H atoms. The bond rearrangement has been observed mostly in neutral molecules

and singly to doubly charged molecular ions [11–13,16–18]. There are fewer reports on the rearrangement of bonds in multiply charged molecules [21,23]; the dissociation of these molecular ions caused by Coulomb repulsion is generally dominant over the process of bond rearrangement. The collisions of highly charged projectiles with  $\text{NH}_3$  can knock out multiple electrons to produce  $\text{NH}_3^{x+}$  ions. Therefore, in the present article, the dissociation of ammonia under the impact of energetic  $\text{H}^+$  and  $\text{Ar}^{q+}$  ( $q = 1, 8$ ) ions is studied, and the dissociation channels of multiply charged ammonia ions with a charge state up to 5 that lead to the formation of  $\text{H}_2^+$  and  $\text{H}_3^+$  are investigated. To elucidate the rearrangement process, *ab initio* intrinsic reaction coordinate (IRC) calculations are performed for doubly charged  $\text{NH}_3$ , and the transition states involved in the formation of  $\text{H}_2^+$  and  $\text{H}_3^+$  are obtained.

**II. EXPERIMENTAL METHOD**

The measurements reported in present article were done at the low-energy ion-beam facility at Inter-University Accelerator Centre, New Delhi, India. The experimental setup is described in detail elsewhere [24,25]. Briefly, energetic highly charged ions (HCIs) are produced using an electron-cyclotron-resonance ion source; the ion species selected for the present experiments are 50 keV  $\text{H}^+$ , 250 keV  $\text{H}^+$ , and 250 keV/ $q$   $\text{Ar}^{q+}$  ( $q = 1, 8$ ). The effusive jet of the target gas ( $\text{NH}_3$ ) is produced using a hypodermic needle. The interaction of the HCIs and the target gas occurs in a high-vacuum chamber. The base pressure of this chamber is maintained at  $2 \times 10^{-8}$  Torr, and it is increased at the most to  $8 \times 10^{-8}$  Torr with the gas load to achieve the single-collision condition. Target-gas density in the interaction zone is of the order of  $10^{12}$   $\text{cm}^{-3}$ , and the diameter of the gas jet is about 2  $\text{mm}^2$ . A time-of-flight (TOF) spectrometer along with a dual-microchannel plate and a position-sensitive delay-line anode is used for the detection of the recoil ions formed due to these interactions; a channeltron is used to detect the ejected electrons. A homogeneous electric field of 500 V/cm is used to guide these recoil ions and electrons towards their respective detectors. The axes of the effusive gas jet, the TOF spectrometer, and the projectile beam are kept mutually perpendicular. The ejected electrons are used as a timing reference for the recoil ions. By measuring the TOF and the position information of the recoil ions produced

\*pbpragya@gmail.com

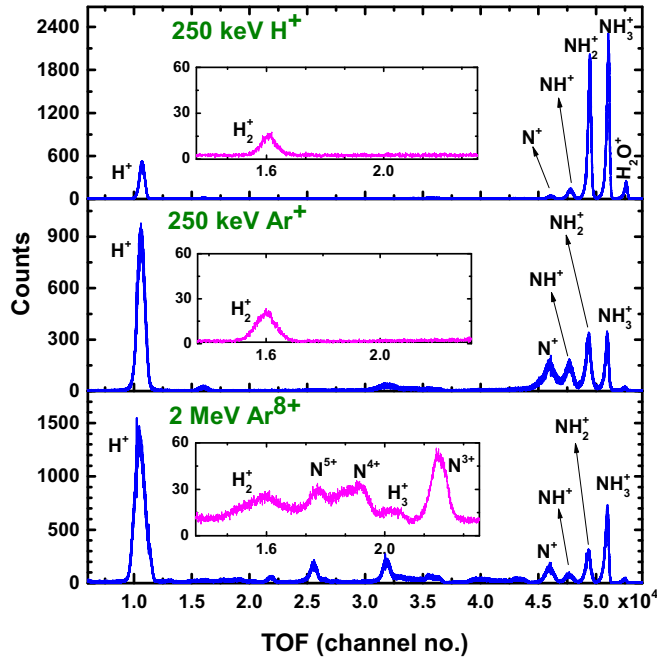


FIG. 1. Time-of-flight spectra of the recoil ions obtained in 250 keV/ $q$   $H^+$  and  $Ar^{q+}$  ( $q = 1, 8$ ) interaction with  $NH_3$ .

in a given collision event, their momenta can be obtained to investigate the dynamical properties of their precursor ion [26]. The projectile ions after colliding with the target gas pass through a parallel-plate electrostatic analyzer and can be detected by another channeltron. In the present study, the charge-state analysis of the postcollision projectile ions is not performed. The TOF spectra generated under the impact of different projectiles are shown in Fig. 1. A typical ion-ion coincidence spectrum obtained for 2 MeV  $Ar^{8+}$  impact on  $NH_3$  is shown in Fig. 2.

### III. RESULTS AND DISCUSSION

The TOF spectra in Fig. 1 show the formation of various recoil ions formed due to dissociation of  $NH_3^{x+}$ . The ions of interest in the present study are  $H_2^+$  and  $H_3^+$ , which are formed due to the bond-rearrangement process. A clear signature of  $H_2^+$  formation is seen for all the projectiles. However, the rearrangement of bonds resulting in  $H_3^+$  is observed only in the case of 2 MeV  $Ar^{8+}$  impact on  $NH_3$ ; we do not have a plausible explanation for this observation at present. At 2 MeV  $Ar^{8+}$  impact four complete dissociation channels (giving rise to only ionic fragments) for  $NH_3^{x+}$  ( $x = 2-5$ ) involving bond rearrangement (see Fig. 2) are seen: (i)  $NH_3^{2+} \rightarrow H_2^+ + NH^+$ , (ii)  $NH_3^{3+} \rightarrow H^+ + H_2^+ + N^+$ , (iii)  $NH_3^{4+} \rightarrow H^+ + H_2^+ + N^{2+}$ , and (iv)  $NH_3^{5+} \rightarrow H^+ + H_2^+ + N^{3+}$ .

The observation of channel (i),  $H_2^+ + NH^+$ , was reported earlier in the literature [12,17,27]. We have observed channels (i-iv) in our experiments. From Fig. 2 it is clear that the  $H_3^+$  ion is not observed in coincidence with nitrogen ions; rather, the dissociation of  $NH_3^+$  gives rise to  $H_3^+$  with a neutral N atom, as seen in the TOF spectrum observed at 2 MeV  $Ar^{8+}$  in Fig. 1. The probability for the bond-rearrangement process is found to be low at the present energies; therefore, the statistics for

the complete dissociation channels (i) to (iv) involving bond rearrangement is poor. However, a qualitative analysis of the dynamics of dissociation is still possible and is presented in Sec. III A.

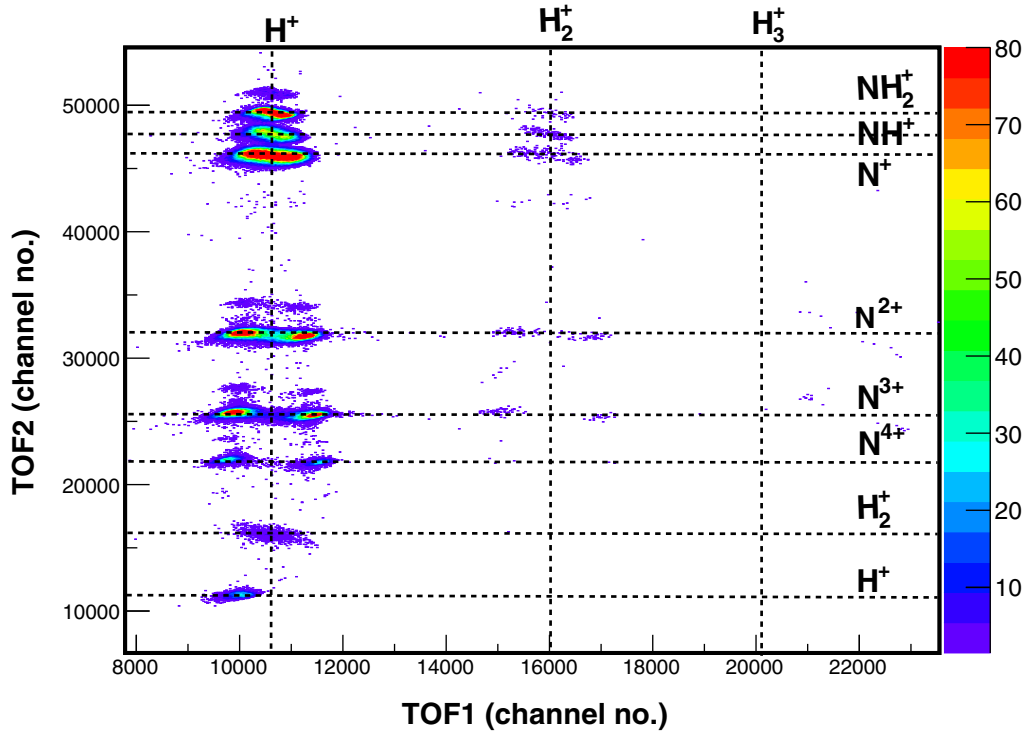
The  $Ar^{8+}$  projectile at 2 MeV has a small time interval to interact with  $NH_3$ ; however, the high charge state of the projectile offers a very high potential field. Therefore, the target molecule experiences the projectile as a rapidly changing electric field. The internal degrees of freedom of the target molecule may be considered to remain frozen during HCI interaction. However, Jochim *et al.* [17] reported rapid formation of  $H_2^+$  and  $H_3^+$  under the impact of 4 MeV  $H^+$  on  $NH_3$  and  $CH_4$ . They concluded that the rearrangement of bonds occurs much faster than the dissociation process. They explained this counterintuitive result using a model which considers the sudden ionization of the molecule followed by a slow dissociation process.

Majima *et al.* [16] observed in single-electron capture and single-electron-loss processes with 580 keV  $C^+$  impact on  $C_2H_6$  that  $H_2^+$  and  $H_3^+$  are formed mostly from doubly charged precursors. Comparing their results with photoionization, they suggested that irrespective of the means of ionization, the  $H_3^+$  ion is generated only from specific excited states of  $C_2H_6^{2+*}$ . Interestingly, in the present observations, the formation of  $H_2^+$  is observed from the  $NH_3^{x+}$  ions having a charge state  $x$  as high as 5, whereas  $H_3^+$  is observed only from the dissociation of  $NH_3^+$ . This implies a certain degree of competition between the bond rearrangement and the Coulomb repulsion processes in  $NH_3^{x+}$ , as discussed for  $NH_3$  and  $CH_4$  under 4 MeV  $H^+$  impact [17], for acetonitrile ( $CH_3CN$ ) in intense laser fields [19], and, recently, for the glycine dications [13] formed under 387.5 keV  $Xe^{25+}$ . However, the H migration is found to contribute only 5%–10% of the total detected processes in latter case. The ultrafast bond rearrangement in  $C_2H_2$  is reported under intense XUV pulses [5]. The rearrangement to result in  $H_3^+$  is also observed in biomolecules by positive-ion impact [28].

#### A. Dissociation dynamics for rearrangement channels

By measuring the relative angles of ejection of the fragment ions, the geometry at the time of dissociation of their precursor can be estimated; however, the changes in the trajectories of the fragment ions caused by the Coulomb repulsion among them might influence the final angular measurements. We have not tried to correct for such angular variations in our measured data. It should be noted here that the angles measured in the present experiments are the asymptotic angles, and these angular distributions can represent, under the recoil approximation [29], information about the orientation of the molecular ion at the instance of collision. The ammonia molecule in its ground state has a trigonal pyramidal geometry and belongs to the  $C_{3v}$  point group with a HNH bond angle of  $107^\circ$ . However, all the low-lying singlet states of  $NH_3$  are planar. Nitrogen has a lone pair of electrons in  $NH_3$ ; tunneling of this lone pair causes rapid nitrogen inversion even at room temperature due to the presence of a narrow and low-energy (0.25 eV) barrier.

To understand the geometry of dissociating  $NH_3^{x+}$ , the scalar triple product of the momentum vectors of its fragment

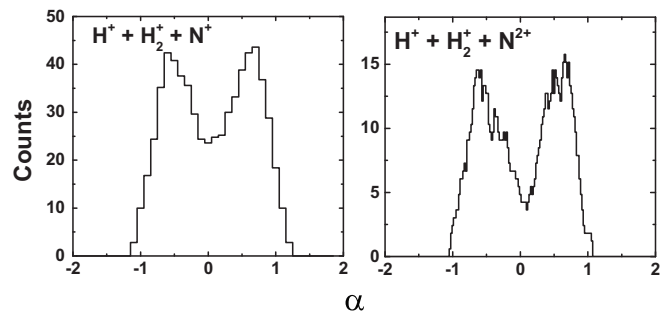

 FIG. 2. Ion-ion coincidence spectrum in 2 MeV  $\text{Ar}^{8+}$  interaction with  $\text{NH}_3$ .

ions is obtained in the laboratory frame. Here, note that in the center-of-mass frame of the molecular ion, the momenta of the fragment ions add to zero and define a dissociation plane. However, the sum of the momenta of the fragments in the laboratory frame may be nonzero if momentum transfer to the center of mass of the molecule as a whole occurred during the collision. The influence of the outgoing highly charged projectile on the dissociating molecular ion has been reported by a few researchers [30,31]. They observed that the heavy projectile collisionally transfers some momentum to the center of mass of the neutral molecule. We define  $\alpha = \hat{p}_{N^{a+}}(\text{lab}) \cdot [\hat{p}_{H^+}(\text{lab}) \times \hat{p}_{H_2^+}(\text{lab})]$  as the coplanarity parameter, where  $\hat{p}_{X^{a+}}(\text{lab})$  is the unit vector parallel to the momentum vector of the fragment ion  $X^{a+}$  measured in the laboratory frame of reference. In the case of coplanar ejection of the three fragments, the distribution of  $\alpha$  will have a peak at zero with a narrow distribution. However, a distribution of  $\alpha$  close to  $\pm 1$  will imply mutually perpendicular emission of the fragments. For dissociation channels (ii) and (iii),  $\alpha$  is plotted in Fig. 3; for  $\text{NH}_3^{5+}$ , the statistics is not sufficient to obtain  $\alpha$ . These distributions are broad and are centered around  $\pm 0.65$ . These results imply that nonplanar dissociation occurs for these channels.

To identify the structure of multiply charged ammonia, consider the angles  $\theta_v$  and  $\chi$  defined in the center-of-mass frame of the molecule [32–34] (see Fig. 4). The velocity of a fragment ion in the center-of-mass frame of its parent molecular ion is defined as  $v_{X^{a+}} = [v_{X^{a+}}(\text{lab}) - v_{\text{CM}}]$ , where  $v_{\text{CM}}$  is the velocity of the center of mass of the molecule and  $v_{X^{a+}}(\text{lab})$  is the fragment ion velocity measured in the laboratory.  $\theta_v$  is the angle between the relative velocity vectors  $(\vec{v}_{N^{a+}} - \vec{v}_{H^+})$  and  $(\vec{v}_{N^{a+}} - \vec{v}_{H_2^+})$ . In dissociation channels

(ii)–(iv) of  $\text{NH}_3^{x+}$  ( $x = 3-5$ ) mentioned above,  $\theta_v$  has a broad distribution centered around  $107^\circ$  (see Fig. 5, left), which is the same as that for the HNH bond angle of neutral  $\text{NH}_3$  within the experimental uncertainties. The angle  $\chi$  (see Fig. 4) between the velocity vectors  $\vec{v}_{N^{a+}}$  and  $(\vec{v}_{H^+} - \vec{v}_{H_2^+})$  gives information about whether the dissociation of the molecular ion occurs in a concerted or stepwise manner. In concerted dissociation, all the bonds break within a time window in which the fragment trajectories evolve under the influence of repulsive forces [33].

For concerted dissociation the angles defined in Fig. 4, in particular  $\cos \chi$ , will be fixed, and its distribution will be a  $\delta$  function [32]. Therefore, the distribution of  $\chi$  will peak at some particular angle. On the other hand, if the dissociation takes place in two steps (i.e., in the first step one bond breaks, and the remaining atoms rotate randomly about their center of mass before dissociating in the second step),  $\cos \chi$  will be uniformly


 FIG. 3. Distribution of coplanarity parameter  $\alpha$  for the dissociation channels  $\text{NH}_3^{3+} \rightarrow \text{H}^+ + \text{H}_2^+ + \text{N}^+$  (left) and  $\text{NH}_3^{4+} \rightarrow \text{H}^+ + \text{H}_2^+ + \text{N}^{2+}$  (right) observed in the 2 MeV  $\text{Ar}^{8+}$  interaction with  $\text{NH}_3$ .

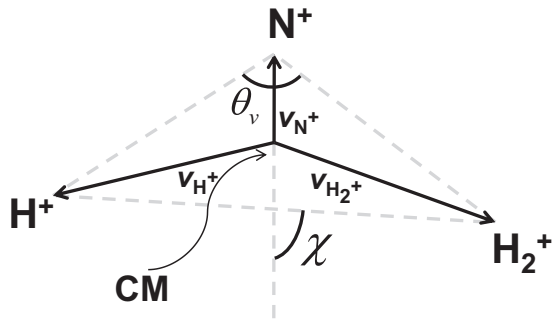


FIG. 4. Definition of the angles  $\theta_v$  and  $\chi$ ; CM represents the center of mass of the system.

distributed; that is, the distribution of  $\chi$  is uniform from  $0^\circ$  to  $180^\circ$ . We observe the angle  $\chi$  to be peaked around  $90^\circ$  (see Fig. 5, right) for dissociation channels (ii)–(iv). These results indicate a rapid bond rearrangement followed by concerted dissociation in multiply charged ammonia ( $\text{NH}_3^{x+}$ ;  $x = 3-5$ ).

Further, the kinetic-energy-release (KER) distributions for dissociation channels (i) to (iv) of  $\text{NH}_3^{x+}$  are obtained and are shown in Fig. 6. KER for a given dissociation event is obtained by summing the individual kinetic energies of the fragments in the molecular center-of-mass frame. The measured KER value gives an estimate for the energy of the precursor molecular ion state that was accessed in the ionizing event; however, it may not be a unique state. Under highly-charged-ion impact, a number of states may be accessed, and therefore, a broad distribution of KER is obtained in our measurements (see Fig. 6). The KER distribution for the two-body dissociation channel  $\text{H}_2^+ + \text{NH}^+$  is shown in Fig. 6; the value reported earlier by Stankiewicz *et al.* [12] under synchrotron radiation of  $200 \text{ \AA}$  is also shown. No other experimental or theoretical

data are available in the literature to compare with our experimental value of KER for this channel.

For comparison with earlier data, we have obtained the KER for a two-body dissociation channel,  $\text{H}^+ + \text{NH}_2^+$ , obtained in the dissociation of  $\text{NH}_3^{2+}$  (see Fig. 6). This channel has been extensively studied in the literature [12,22,35]. The previously reported experimental values of the KERs in the literature are also shown in Fig. 6. Comparison with the earlier data indicates that the high-lying states ( $^1E$  and above) of  $\text{NH}_3^{2+}$  are dominantly populated in our measurements. In most of the previous results for  $\text{NH}_3^{2+}$  dissociating into  $\text{H}^+ + \text{NH}_2^+$ , the states involving only vertical transitions within the Franck-Condon region are considered, which means the geometry of these doubly charged molecular ionic states is the same as that of neutral  $\text{NH}_3$ . In earlier works, the electronic states of  $\text{NH}_3^{2+}$  were measured using auger spectroscopy [35], double-charge-transfer spectroscopy [36], mass spectrometry [37], translational energy spectroscopy [38], and photoion-photoion coincidence [22]. The theoretically calculated states of  $\text{NH}_3^{2+}$  are also available and are reported to lie within 33.5 to 46.8 eV above the energy of the ground state of  $\text{NH}_3$  [36,39–43].

For dissociation channels (ii) to (iv), which are obtained from the dissociation of multiply charged  $\text{NH}_3^{x+}$  ( $x = 3-5$ ) ions into  $\text{H}^+ + \text{H}_2^+ + \text{N}^{a+}$  ( $a = 1-3$ ), the nitrogen ion  $\text{N}^{a+}$  gets a very small kinetic energy, whereas the proton and the molecular hydrogen ion fly away with larger kinetic energies. There are no experimental or theoretical results available to compare the results of KERs for  $\text{NH}_3^{x+}$  ( $x = 3-5$ ). In multiply charged molecular ions, the Coulomb repulsion between the constituent atoms is very high because of the excess positive charge, and this results in prompt dissociation of the molecular ion. In such cases, KERs can be estimated by considering the point-charge approximation of Coulomb explosion (CE) model [34]. This model considers the charges on atoms to be pointlike, situated at their equilibrium distances in the

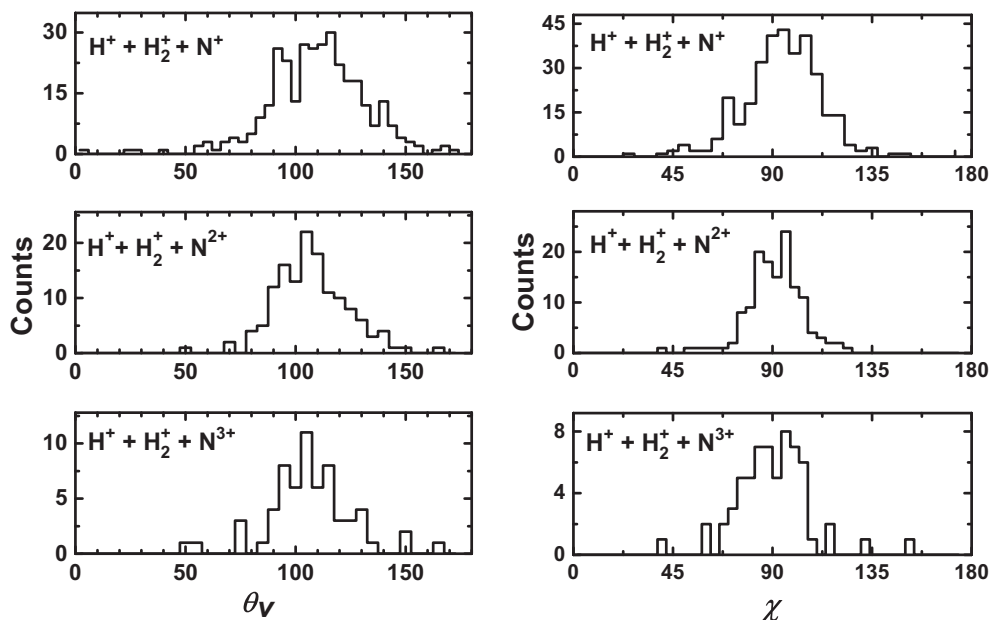


FIG. 5. Distribution of  $\theta_v$  (left) and  $\chi$  (right) for the three-body dissociation channels of  $\text{NH}_3^{x+}$  ( $x = 3-5$ ) obtained in the interaction of  $2 \text{ MeV Ar}^{8+}$  with  $\text{NH}_3$ .

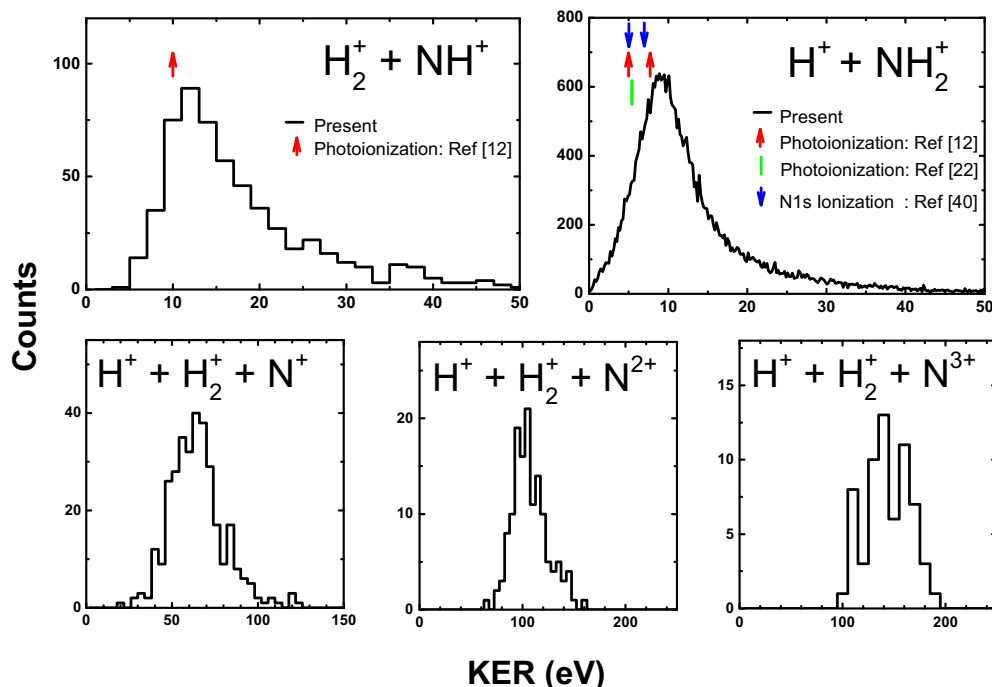


FIG. 6. Distribution of kinetic-energy release in different dissociation channels of  $\text{NH}_3^{x+}$  ( $x = 2-5$ ) involving the rearrangement of hydrogen atoms for interaction of 2 MeV  $\text{Ar}^{8+}$  with  $\text{NH}_3$ .

precursor. However, in the case of bond rearrangement in a multiply charged precursor, it is difficult to get an idea about the equilibrium distances among its constituents. If we assume that the bond rearrangement in  $\text{NH}_3^{x+}$  occurs in a linear geometry as  $\text{H-N-H}_2$ , KER values of 50.3, 91.4, and 132.6 eV will be obtained from the CE model for channels (ii)–(iv), respectively. In the present case, we have observed very high values of KER for  $\text{NH}_3^{x+}$  ( $x = 3-5$ ) compared to the dication channels (see Fig. 6). The rearrangement of bonds in multiply charged  $\text{NH}_3$  and high values of KER observed indicate an ultrafast rearrangement of atoms followed by dissociation of the precursor. We have obtained classically the dissociation time for the N-H bond to get an estimate for the time available for bond rearrangement. Using the CE model, we have obtained the time for the N-H internuclear distance to increase to twice its initial value to be of the order of femtoseconds in a very crude approximation [44]. The ultrafast H-atom migration was reported earlier in monocations and dications of ammonia [17] and methane [17], glycine dications [13], and acetonitrile dications [19].

### B. IRC calculations

In an attempt to understand the bond rearrangement in  $\text{NH}_3$ , we performed *ab initio* IRC calculations for the doubly charged  $\text{NH}_3$  dissociating via three different pathways, namely,  $\text{H}^+ + \text{NH}_2^+$ ,  $\text{H}_2^+ + \text{NH}^+$ , and  $\text{H}_3^+ + \text{N}^+$  (see Figs. 7–9). The calculations were done at the unrestricted Hartree-Fock level under adiabatic approximation. Starting from the optimized transition state (i.e., the ground-state  $\text{NH}_3^{2+}$ ), the IRC calculations were done using the quantum chemistry package GAMESS [45]; the correlation-consistent polarized valence

double zeta (cc-PVDZ) basis set was used. We have not made any attempt to obtain the PES of the dissociating  $\text{NH}_3^{2+}$  ions; however, we have tried to find out the existence, if any, of a potential barrier that may be present for the rearrangement of H atoms in doubly ionized  $\text{NH}_3$ . We have observed in our calculations that for rearrangement to occur,  $\text{NH}_3^{2+}$  should have a planar geometry rather than the trigonal pyramidal shape. Therefore, from here on, we discuss only the planar geometry (also reported in [46,47]) for the precursor  $\text{NH}_3^{2+}$  in our calculations.

First, we obtained a transition state for planar  $\text{NH}_3^{2+}$  dissociating into  $\text{H}^+ + \text{NH}_2^+$  (Fig. 7) and having a potential barrier of 1.9 eV to be consistent with the earlier results [12,48].

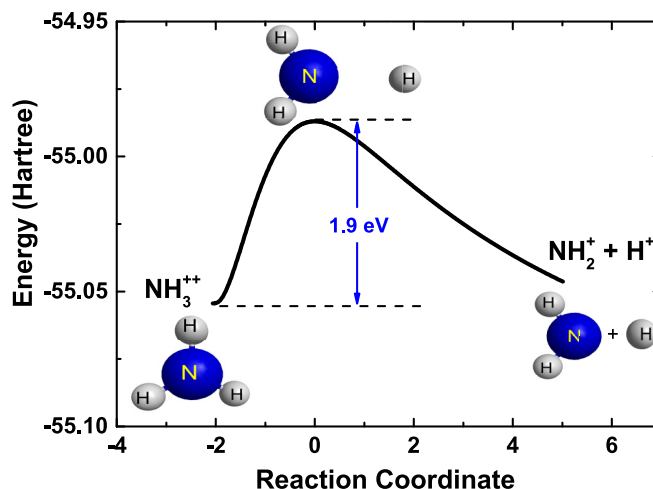


FIG. 7. Reaction path for the dissociation of  $\text{NH}_3^{2+}$  into  $\text{H}^+ + \text{NH}_2^+$  considering the initial geometry to be planar.

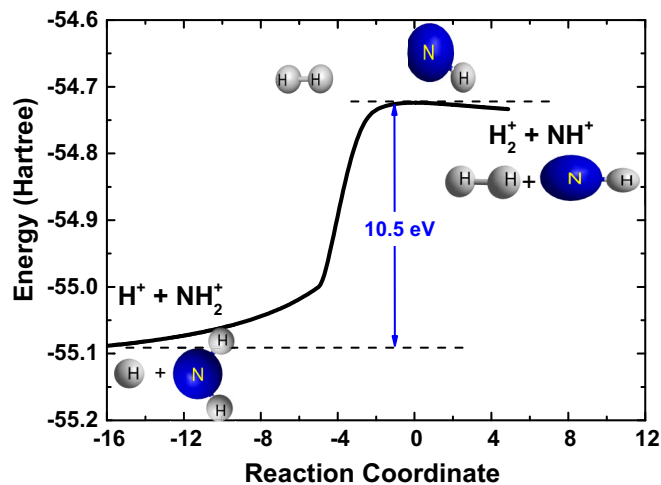


FIG. 8. Reaction path for the formation of  $\text{H}_2^+ + \text{NH}^+$  from  $\text{H}^+ + \text{NH}_2^+$ .

Walsh *et al.* [27] studied the states of  $\text{NH}_3^{2+}$  dissociating into  $\text{H}^+ + \text{NH}_2^+$  by core ionization around N  $1s$  excitation to  $4a_1$  in  $\text{NH}_3$ . They observed that if the excitation is to a bound part of the PES, the molecule has a longer time to relax to a planar geometry, and if the core excitation is to a steep unbound part of the PES, the molecule dissociates on a femtosecond time scale while having its ground-state geometry. From our experimental and theoretical work, we cannot affirm the time scale of bond rearrangement and dissociation in the case of dications of  $\text{NH}_3$ . However, for higher charged states of  $\text{NH}_3^{x+}$  ( $x = 3-5$ ), our experimental results indicate ultrafast bond rearrangement in competition with Coulomb explosion, as discussed in Sec. III A.

The IRC path for the formation of  $\text{H}_2^+$  is not obtained from  $\text{NH}_3^{2+}$ ; rather, it is obtained along the path from  $\text{H}^+ + \text{NH}_2^+$  which may be possible if the  $\text{NH}_3^{2+}$  precursor follows another reaction path which has a transition state with a broad potential barrier giving rise to the bond rearrangement channel  $\text{H}_2^+ + \text{NH}^+$  (Fig. 8). The IRC here is a combination of N-H bond lengths and H-N-H bond angles, whereas in Fig. 7 the intrinsic parameter is the N-H bond length throughout the path except for a small contribution from the H-N-H bond angle near the transition state. Along the IRC path in Fig. 8,  $\text{NH}_2^+$  rotates slowly, and the bond length  $r_1$  between N and one of the H atoms (say, H1) attached to it increases rapidly, and H1 starts to form a bond with the free  $\text{H}^+$ . At the transition state,  $r_1$  is about 2 Å, which further increases along this path and results in the separation of  $\text{NH}^+$  and  $\text{H}_2^+$ . The sudden change in slope in Fig. 8 around an IRC of  $-5$  cannot be explained by our calculations, which were done under adiabatic approximation. Therefore, the existence of a curve crossing or a funnel structure in the PES of  $\text{NH}_3^{2+}$  cannot be ruled out for the rearrangement channel  $\text{H}_2^+ + \text{NH}^+$ . Nonadiabatic calculations are needed to verify such curve crossing phenomena. The reaction path obtained using the IRC calculation connects the transition state to the precursor ( $\text{NH}_3^{2+}$ ) and to the products. Our calculations show that the transition state for the  $\text{H}_2^+$  formation channel is much higher in energy than that of the  $\text{H}^+ + \text{NH}_2^+$  dissociation pathway.

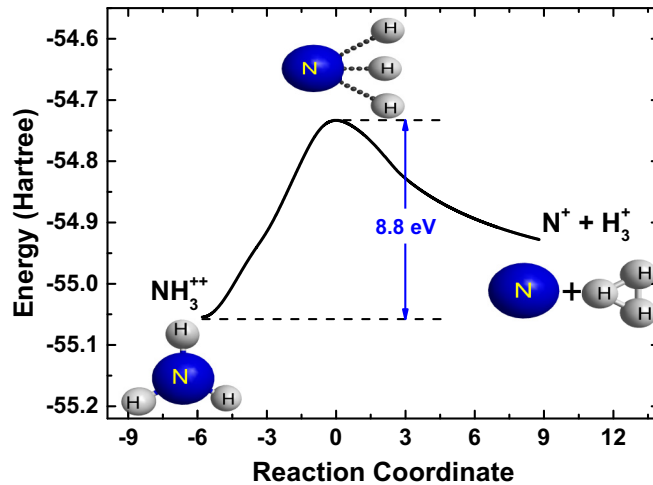


FIG. 9. Reaction path for the dissociation of  $\text{NH}_3^{2+}$  into  $\text{H}_3^+ + \text{N}^+$  considering the initial geometry to be planar.

The rearrangement of three H atoms to form  $\text{H}_3^+$  is observed in our experiments from only  $\text{NH}_3^+$ , with very low probability [see the single-ion coincidence (TOF) spectrum, Fig. 1]. We could not obtain the transition state for the formation of  $\text{H}_3^+$  from  $\text{NH}_3^+$  in our IRC calculations. However, Jochim *et al.* [17] calculated the PES for  $\text{NH}_3^+$  dissociating into  $\text{H}_3^+$  and neutral N. They considered only the symmetric stretch configuration of the  $\text{H}_3^+$  triangle away from the nitrogen atom which gives rise to two different reaction paths with potential barriers at 4.35 and 11 eV, respectively.

To account for the absence of the  $\text{H}_3^+ + \text{N}^+$  channel in our double-ion coincidence spectrum shown in Fig. 2, we performed IRC calculations for  $\text{H}_3^+$  formation from  $\text{NH}_3^{2+}$ , and the results are shown in Fig. 9. The optimized geometry for the precursor ion  $\text{NH}_3^{2+}$  is found to be planar for observing the formation of  $\text{H}_3^+$  with  $\text{N}^+$ . The precursor ion rearranges itself, and while following the minimum-energy path, it passes through a transition state. The potential barrier offered is 8.8 eV. At the transition state, a very distinct feature is seen from the other dissociation pathways of  $\text{NH}_3^{2+}$  in which the precursor reorients itself, so that the three H atoms become colinear while still being attached to the N atom, and at the end of this path all three H atoms are separated from the nitrogen atom, giving rise to the coincidence channel  $\text{H}_3^+ + \text{N}^+$ . The geometries at different points of the reaction path are also shown. We have calculated the electron densities for the precursor and its products to verify that  $\text{H}_3^+$  is formed. The separation between any two H atoms in  $\text{H}_3^+$  is found to be 0.88 Å, with the geometry of  $\text{H}_3^+$  being equilateral. Our calculations suggest that the requirement of a specific geometrical arrangement at the transition state apart from the potential barrier of 8.8 eV might be responsible for the absence of the dissociation channel  $\text{H}_3^+ + \text{N}^+$  in our ion-ion coincidence spectrum (Fig. 2).

#### IV. CONCLUSIONS

Under energetic ion impact on  $\text{NH}_3$ , the rearrangement process of hydrogen atoms was studied. The rearrangement

to result in  $\text{H}_2^+$  was observed in the case of singly to multiply charged  $\text{NH}_3^{x+}$  ( $x \leq 5$ ) precursors. However,  $\text{H}_3^+$  is obtained only from singly charged  $\text{NH}_3$  in our experiments. The coincidence channels  $\text{H}^+ + \text{H}_2^+ + \text{N}^{a+}$  ( $a = 1-3$ ) were observed. Our experimental data further suggest that there is a competition between Coulomb explosion and bond-rearrangement processes for the dissociation of multiply charged  $\text{NH}_3^{x+}$  ( $x = 3-5$ ) ions. The *ab initio* calculations suggest that the rearrangement of bonds in  $\text{NH}_3^{2+}$  to result in  $\text{H}_2^+$  and  $\text{H}_3^+$  requires the initial geometry of the precursor ion to be planar; it should be noted that neutral  $\text{NH}_3$  has a trigonal pyramidal structure. The transition state for the formation of  $\text{H}_3^+$  from  $\text{NH}_3^{2+}$  demands the three H atoms become colinear while all of them are attached to the N atom, and the potential barrier is as high as 8.8 eV for this path. It may be concluded that the rearrangement of hydrogen atoms, although having low probability, is possible at present energies. Further studies

considering separately the electron capture and the ionization processes are required to elucidate the effect of the interaction strength on the formation probability of ions, in particular for the ions formed in bond-rearrangement processes. Further, the substitution of one or more hydrogen atoms (e.g., isotope labeling) could be helpful to study this process.

#### ACKNOWLEDGMENTS

The low-energy ion-beam facility staff at IUAC is gratefully acknowledged for their cooperation during the experiments. P.B. acknowledges the Department of Science and Technology, New Delhi, India, for support through an INSPIRE Faculty grant (Grant No. IFA14/PH-89). T.S. gratefully acknowledges the University Grants Commission, New Delhi, for providing financial support in the form of a fellowship.

- 
- [1] P. I. Nagy, *Int. J. Mol. Sci.* **15**, 19562 (2014).
- [2] L. Antonov, *Tautomerism: Concepts and Applications in Science and Technology* (Wiley, Hoboken, NJ, 2016).
- [3] M. A. Bellucci and D. F. Coker, *J. Chem. Phys.* **136**, 194505 (2012).
- [4] D. K. Bohme, *Int. J. Mass Spectrom. Ion Processes* **115**, 95 (1992).
- [5] Y. Jiang, A. Rudenko, O. Herrwerth, L. Foucar, M. Kurka, K. Kühnel, M. Lezius, M. F. Kling, J. van Tilborg, A. Belkacem *et al.*, *Phys. Rev. Lett.* **105**, 263002 (2010).
- [6] M. Kübel, R. Siemering, C. Burger, N. G. Kling, H. Li, A. S. Alnaser, B. Bergues, S. Zhrebtsov, A. M. Azzeer, I. Ben-Itzhak, R. Moshhammer, R. de Vivie-Riedle, and M. F. Kling, *Phys. Rev. Lett.* **116**, 193001 (2016).
- [7] M. Garg, A. K. Tiwari, and D. Mathur, *J. Chem. Phys.* **136**, 024320 (2012).
- [8] J. E. Dyson and D. A. Williams, *The Physics of the Interstellar Medium* (Taylor & Francis, New York, 1997).
- [9] H. Rauchfuss, *Chemical Evolution and the Origin of Life* (Springer, Berlin, 2008).
- [10] D. E. Newton, *Chemistry of Space* (Facts on File Inc., New York, 2007).
- [11] J. Laksman, E. P. Månsson, A. Sankari, D. Céolin, M. Gisselbrecht, and S. L. Sorensen, *Phys. Chem. Chem. Phys.* **15**, 19322 (2013).
- [12] M. Stankiewicz, P. Hatherly, L. Frasinski, K. Codling, and D. Holland, *J. Phys. B* **22**, 21 (1989).
- [13] S. Maclot, D. G. Piekarski, A. Domaracka, A. Mery, V. Vizcaino, L. Adoui, F. Martín, M. Alcamí, B. A. Huber, P. Rousseau *et al.*, *J. Phys. Chem. Lett.* **4**, 3903 (2013).
- [14] S. Kaziannis, I. Lontos, G. Karras, C. Corsi, M. Bellini, and C. Kosmidis, *J. Chem. Phys.* **131**, 144308 (2009).
- [15] M. N. Piancastelli, A. Hempelmann, F. Heiser, O. Gessner, A. Rüdél, and U. Becker, *Phys. Rev. A* **59**, 300 (1999).
- [16] T. Majima, T. Murai, T. Kishimoto, Y. Adachi, S. O. Yoshida, H. Tsuchida, and A. Itoh, *Phys. Rev. A* **90**, 062711 (2014).
- [17] B. Jochim, A. Lueking, L. Doshier, S. Carey, E. Wells, E. Parke, M. Leonard, K. Carnes, and I. Ben-Itzhak, *J. Phys. B* **42**, 091002 (2009).
- [18] S. Sorensen, M. Gisselbrecht, J. Laksman, E. Månsson, D. Céolin, A. Sankari, and F. Afaneh, *J. Phys. Conf. Ser.* **488**, 012006 (2014).
- [19] A. Hishikawa, H. Hasegawa, and K. Yamanouchi, *J. Electron Spectrosc. Relat. Phenom.* **141**, 195 (2004).
- [20] S. De, J. Rajput, A. Roy, P. N. Ghosh, and C. P. Safvan, *Phys. Rev. Lett.* **97**, 213201 (2006).
- [21] M. Krishnamurthy, F. Rajgara, and D. Mathur, *J. Chem. Phys.* **121**, 9765 (2004).
- [22] D. Winkoun and G. Dujardin, *Z. Phys. D* **4**, 57 (1986).
- [23] I. Ben-Itzhak, A. M. Saylor, M. Leonard, J. Maseberg, D. Hathiramani, E. Wells, M. Smith, J. Xia, P. Wang, K. Carnes *et al.*, *Nucl. Instrum. Methods Phys. Res., Sect. B* **233**, 284 (2005).
- [24] S. De, P. Ghosh, A. Roy, and C. Safvan, *Nucl. Instrum. Methods Phys. Res., Sect. B* **243**, 435 (2006).
- [25] A. Kumar, J. Rajput, T. Sairam, M. Jana, L. Nair, and C. Safvan, *Int. J. Mass Spectrom.* **374**, 44 (2014).
- [26] I. Ali, R. Dörner, O. Jagutzki, S. Nüttgens, V. Mergel, L. Spielberger, K. Khayyat, T. Vogt, H. Bräuning, K. Ullmann *et al.*, *Nucl. Instrum. Methods Phys. Res., Sect. B* **149**, 490 (1999).
- [27] N. Walsh, A. Sankari, J. Laksman, T. Andersson, S. Oghbaie, F. Afaneh, E. P. Månsson, M. Gisselbrecht, and S. L. Sorensen, *Phys. Chem. Chem. Phys.* **17**, 18944 (2015).
- [28] S. Bari, P. Sobocinski, J. Postma, F. Alvarado, R. Hoekstra, V. Bernigaud, B. Manil, J. Rangama, B. Huber, and T. Schlathölter, *J. Chem. Phys.* **128**, 074306 (2008).
- [29] R. N. Zare, *J. Chem. Phys.* **47**, 204 (1967).
- [30] F. Frémont, C. Bedouet, M. Tarisien, L. Adoui, A. Cassimi, A. Dubois, J. Chesnel, and X. Husson, *J. Phys. B* **33**, L249 (2000).
- [31] R. D. DuBois, I. Ali, C. L. Cocke, C. R. Feeler, and R. E. Olson, *Phys. Rev. A* **62**, 060701(R) (2000).
- [32] C. Strauss and P. L. Houston, *J. Phys. Chem.* **94**, 8751 (1990).
- [33] S. Hsieh and J. H. Eland, *J. Phys. B* **30**, 4515 (1997).
- [34] B. Siegmann, U. Werner, H. O. Lutz, and R. Mann, *J. Phys. B* **35**, 3755 (2002).
- [35] C. Ma, D. Hanson, K. Lee, and R. G. Hayes, *J. Electron Spectrosc. Relat. Phenom.* **75**, 83 (1995).
- [36] J. Appell and J. Horsley, *J. Chem. Phys.* **60**, 3445 (1974).

- [37] T. Märk, F. Egger, and M. Cheret, *J. Chem. Phys.* **67**, 3795 (1977).
- [38] R. Locht and J. Momigny, *Chem. Phys. Lett.* **138**, 391 (1987).
- [39] F. Tarantelli, A. Tarantelli, A. Sgamellotti, J. Schirmer, and L. Cederbaum, *Chem. Phys. Lett.* **117**, 577 (1985).
- [40] M. T. Økland, K. Fægri, and R. Manne, *Chem. Phys. Lett.* **40**, 185 (1976).
- [41] D. R. Jennison, *Phys. Rev. A* **23**, 1215 (1981).
- [42] R. Boyd, S. Singh, and J. Beynon, *Chem. Phys.* **100**, 297 (1985).
- [43] W. Griffiths and F. Harris, *Rapid Commun. Mass Spectrom.* **4**, 366 (1990).
- [44] I. Last, I. Schek, and J. Jortner, *J. Chem. Phys.* **107**, 6685 (1997).
- [45] M. W. Schmidt, K. K. Baldrige, J. A. Boatz, S. T. Elbert, M. S. Gordon, J. H. Jensen, S. Koseki, N. Matsunaga, K. A. Nguyen, S. Su *et al.*, *J. Comput. Chem.* **14**, 1347 (1993).
- [46] A. Walsh, *J. Chem. Soc.* 2296 (1953).
- [47] B. D. Joshi, *J. Chem. Phys.* **46**, 875 (1967).
- [48] S. A. Pope, I. H. Hillier, M. F. Guest, and J. Kendrick, *Chem. Phys. Lett.* **95**, 247 (1983).